Journal of Molecular Structure 1102 (2015) 101–107

Contents lists available at ScienceDirect

Journal of Molecular Structure

journal homepage: http://www.elsevier.com/locate/molstruc

New class of bicyclic compounds derived from thiobarbituric acid with representative compound 1,3-diethyl-7-hydroxy-5,5,7-trimethyl-2-thioxo-1,2,3,5,6,7-hexahydro-4H-pyrano[2,3-d]pyrimidin-4-one. Preparation, crystal structure, mass spectrometry and IR spectroscopy

Nicolay N. Golovnev [a], Maxim S. Molokeev [b, c, *], Irina V. Sterkhova [d], Yuriy V. Goryunov [a], Victor V. Atuchin [e, f, g, h]

[a] Siberian Federal University, Svobodny Aven. 79, Krasnoyarsk 660041, Russia
[b] Kirensky Institute of Physics, SB RAS, Akademgorodok 50, Bld. 38, Krasnoyarsk 660036, Russia
[c] Far Eastern State Transport University, 47 Serysheva Str., Khabarovsk 680021, Russia
[d] Laboratory of Physical Chemistry, Irkutsk Favorsky Institute of Chemistry, SB RAS, 1 Favorsky, Irkutsk 664033, Russia
[e] Laboratory of Optical Materials and Structures, SB RAS, Institute of Semiconductor Physics, 13 Lavrentiev Aven., Novosibirsk 630090, Russia
[f] Functional Electronics Laboratory, Tomsk State University, 36 Lenin Aven., Tomsk 634050, Russia
[g] Laboratory of Semiconductor and Dielectric Materials, Novosibirsk State University, 2 Pirogov Str., Novosibirsk 630090, Russia
[h] Institute of Thermophysics, 1 Lavrentiev Aven., Novosibirsk 630090, Russia

ARTICLE INFO

Article history:
Received 16 June 2015
Received in revised form
13 August 2015
Accepted 19 August 2015
Available online 24 August 2015

Keywords:
Bicyclic compounds
Thiobarbiturates
Heterocycles
X-ray diffraction
IR spectroscopy
Theoretical calculations

ABSTRACT

The colorless crystals of 1,3-diethyl-7-hydroxy-5,5,7-trimethyl-2-thioxo-1,2,3,5,6,7-hexahydro-4H-pyrano[2,3-d]pyrimidin-4-one (**1**) have been crystallized from the solution containing 1,3-diethyl-2-thiobarbituric acid (HDETBA) and equal volumes of concentrated HCl and acetone A possible stoichiometric reaction mechanism has been suggested. The crystal structure of **1** has been determined by X-ray single crystal analysis. The phase purity of the precipitate has been verified by powder X-ray diffraction analysis. Compound **1** crystallizes in the orthorhombic structure, space group $P2_12_12_1$, with cell parameters $a = 9.7454(4)$, $b = 11.2225(4)$, $c = 13.9171(5)$ Å, $Z = 4$, $V = 1522.1(1)$ Å^3. The molecules of **1** contain the bicyclic ring constructions new in thiobarbiturates. The molecules of **1** are linked by O—H···O hydrogen bonds to infinite molecule chains. The results of mass spectrometric analysis, theoretical studies and IR spectroscopy confirm the structure of **1**. Using the PASS software, the general pharmacological potential of **1** was analyzed.

1. Introduction

Thiobarbiturates are valuable compounds for different pharmacological applications, such as general anesthesia, sedation and anticonvulsant effects [1]. Thiobarbituric acid derivatives also exhibited antimicrobial [2], antifungal [3], antiviral [4], and antitumor activities [5]. They show diverse biological activities, such as antituberculosis [6], anticancer with anti-inflammatory activities [7] and urease inhibition [8]. Despite the widespread use of 2-thiobarbituric acid (H_2TBA) and its derivatives, their possible transformations with parallel participation of several functional groups in organic solutions were not well understood. However, the presence of an active methylene group ($C5H_2$) and two adjacent reactive carbonyl groups suggests the possibility of thiobarbiturate compounds formation, including bicyclic ones, for example when they interact with ketones.

The biological activity of the compounds depends on the acid–base properties. Earlier, it was shown that thiobarbituric acids are protonated in acidic media and form singly charged cations, although the respective crystal salts were still not obtained [9–11]. Originally, a reaction of the most available reagents H_2TBA, HDETBA and HCl was considered to form such salts. HCl was selected due to its strong acidic properties, non-oxidizing nature and widespread availability. A new organic derivative of HDETBA with interesting structure formations and physical properties is explored in the

* Corresponding author. Kirensky Institute of Physics, SB RAS, Bld. 38 Akademgorodok 50, Krasnoyarsk 660036, Russia.
E-mail address: msmolokeev@gmail.com (M.S. Molokeev).

http://dx.doi.org/10.1016/j.molstruc.2015.08.046
0022-2860/

present work; compound **1** is occasionally found in the attempt to get an interaction product of 1,3-diethyl-2-thiobarbituric acid with a concentrated HCl solution by salting it with acetone. Under similar conditions, the unidentified multiphase product was obtained by reacting acetone with H_2TBA. As it is found, the bicyclic HDETBA-based compound may exhibit pharmacological activity. Presently, HDETBA is used in nonlinear optics materials [12,13], for chromatographic determination of nicotine and its urinary metabolites [14] and as an alternative coinitiator for acidic photopolymerizable dental materials [15].

2. Experimental section

2.1. Chemical reagents

1,3-diethyl-2-thiobarbituric acid (Sigma–Aldrich, CAS No. 110871-86-8, with ≥98.0% of purity), acetone, HCl and KBr were of analytical grade and were supplied from Acros. All the chemicals were used as received, without any further purification.

2.2. Synthesis

1,3-diethyl-7-hydroxy-5,5,7-trimethyl-2-thioxo-1,2,3,5,6,7-hexahydro-4H-pyrano[2,3-d]pyrimidin-4-one (**1**) has been crystallized by reacting 1,3-diethyl-2-thiobarbituric acid with acetone in the presence of HCl. Compound **1** was prepared by mixing 5 mL of acetone, 200 mg of HDETBA and 2 mL concentrated HCl in arbitrary order. Colorless needle-like single crystals suitable for X-ray analysis were grown by continuous evaporation of the filtrate during few weeks in ambient conditions. They were separated from the solution by filtering, washed by a small amount of acetone and dried in the air at room temperature. The crystals suitable for X-ray analysis were selected from the precipitate. The final product output was about 50%. The powder product **1** was sparingly soluble in water but more soluble in alcohol and acetone. The compound has the melting point of 137 °C. The chemical analysis of **1** was carried out with a HCNS-0 EA 1112 Flash Elemental Analyser. The elemental analysis for $C_{14}H_{22}N_2O_3S$: Calc.: C, 56.4%; H, 7.43%; N, 9.39%; S, 10.8. Found: C, 56.7%; H, 7.62%; N, 9.57%; S, 11.0%. The powder pattern of **1** simulated from the single crystal structural data well agrees with the measured one (Fig. 1S) indicating that the crystal structure is representative of the bulk structure.

2.3. Physical measurements

The IR spectra of crystalline samples of **1** (in KBr) and its solutions in CCl_4 (in CaF_2 cuvette) were measured on a Varian 3100 FTIR spectrometer. The spectral resolution during measurements was 5 cm^{-1}.

The powder X-ray diffraction data were obtained using the D8 ADVANCE (Bruker) diffractometer equipped with a VANTEC detector and a Ni filter. The measurements were produced using Cu Kα radiation. The peak positions were determined using the EVA program (2004 release) from the Bruker DIFFRAC-PLUS software.

To obtain the structural parameters, a colorless crystal 0.41 × 0.23 × 0.22 mm in size was studied at 24 °C. The reflection intensities were measured on a SMART APEX II single crystal diffractometer (Bruker AXS) equipped with a CCD-detector, graphite monochromator and Mo Ka radiation source. The absorption corrections were applied using the SADABS program by the multiscan method.

The UV–Vis spectra in the aqueous solution were measured with an Evolution 300 scanning spectrophotometer (Thermo-Scientific, England) using 1 cm quartz cells. Chromato-mass-spectroscopic analyses were conducted on a chromatograph Agilent Technologies 7890 A with quadrupole mass MSD 5975 C as a detector using a 30 m quartz column HP-5 (copolymer 5%-diphenyl – 95%-dimethylsiloksan) with the inner diameter of 0.25 mm. The evaporator and ion source temperatures were 280 and 173 °C, respectively, and helium was used as a carrier gas at the flow of 1 mL/min. The column temperature was 50 °C (2 min); then the temperature was increased over the range of 50–270 °C at the rate of 4 °C/min, and the isothermal stage was being realized at 270 °C for 10 min. Compound **1** was analyzed in an ethanol solution.

3. Results and discussion

3.1. Synthesis of *1*

New compound **1** was prepared by the reaction of 1,3-diethyl-2-thiobarbituric acid with acetone at the addition of HCl. Probably, one of its stages is a condensation reaction of Knoevenagel [16]. The HDETBA molecules in the crystaline state are present in the enol form [17,18]. However, in solutions, for example in CH_3OH or in the mixture of DMSO and D_2O, keto and enol forms coexist in equilibrium [19], and each of them could participate in the condensation and other reactions. The reaction steps could be presented by Scheme 1.

Acetone reacts with the C5 atom of 2-thiobarbituric acids [20] or

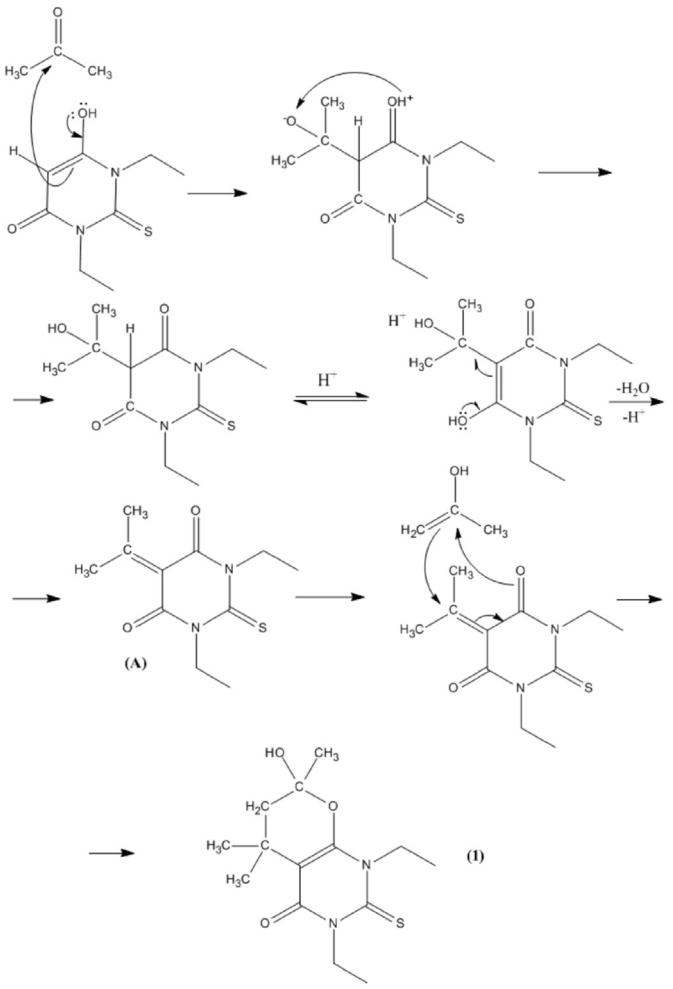

Scheme 1. The path through the formation of the reaction intermediate 5-(isopropylidene)-2-thiobarbituric acid.

with their 1-N-aryl substituents [21] by the same way as it is expected for the compounds with an active methylene group. This yields the corresponding 5-isopropylidene derivatives. Similarly, the evaporation of acetone solution of barbituric acid yielded the plate-like crystals of 5-(isopropylidene)-barbituric acid [22]. Therefore, it was supposed, that 5-(isopropylidene)-1,3-diethyl-2-thiobarbituric acid (Scheme 1, product A) can be the intermediate compound during the formation of bicyclic compound **1**. It was supposed that hydrogen ions are the catalyst of acetone enolization [16]. Partial acetone enolization occurs in an acidic environment, and the closure of the heterocycle happens during its interaction with a molecule of 5-(isopropylidene)-1,3-diethyl-2-thiobarbituric acid.

Besides, the liquid phase, in the form of orange droplets, has been formed in the non-acidified aqueous acetone solution at 60 °C during 6–8 h. The droplets coalesced upon cooling of the two-phase system down to 5 °C, and, on further storing, the orange crystal mixture mainly consisting of **1**, HDETBA and a small amount of unidentified impurity was crystallized. Thus, generally, the formation of **1** is possible without HCl introduction. In the reactive mixture, which was kept at room temperature during several weeks, the resinous products, which were not investigated, additionally formed. Supposedly, the products formation appeared due to the participation of end OH-group of compound **1** in a subsequent condensation reaction with acetone and/or with HDETBA.

3.2. The crystal structure of *1*

The structure was solved by direct methods and subsequent difference Fourier synthesis, and was refined using the SHELXTL software package [23,24]. All non-hydrogen atoms were refined anisotropically. Partly, hydrogen atoms were located from the Fourier maps, and all other hydrogen atoms were added in calculated positions. The crystallographic data for the compound **1** are summarized in Table 1. The asymmetric part of the **1** unit cell contains one $C_{14}H_{22}N_2O_3S$ molecule (Fig. 1). Bond length d(C5–C11) = 1.521(3) Å is similar to the single bond d(C5–C7) = 1.551(4) Å between similar atoms in 5-(isopropyl)-2-thiobarbituric acid [25] and is noticeably longer than the double bond of d(C5–C7) = 1.363(4) Å in 5-(isopropylidene)-2-thiobarbituric acid [20]. Thus, this bond in **1** should be classified as a single one. Bond length d(O1–C4) = 1.340(3) Å is noticeably longer than d(O2–C6) = 1.241(3) Å (Table 2) and, therefore, these can be classified as single and double bonds, respectively. Previously, such difference of bond lengths (d(O1–C4) = 1.264 Å, d(O2–C6) = 1.312 Å) was also observed in the HDETBA compound [17,18]. The metal complexes with $DETBA^-$ [26–28], however, show the charge delocalization in the O=C–CH–C=O group and very similar lengths of O1–C4 and O2–C6 bonds.

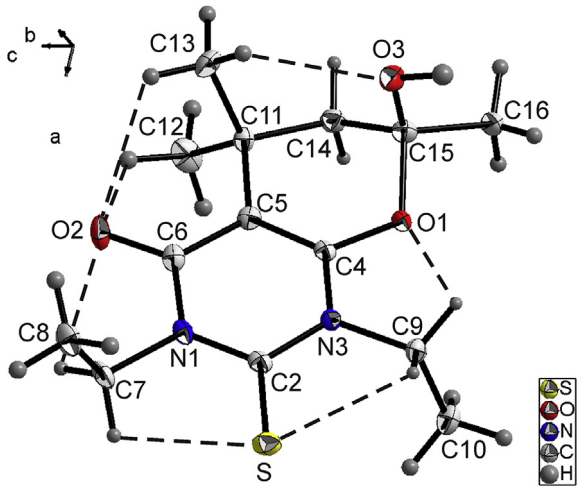

Fig. 1. The independent part of the unit cell of **1**. The ellipsoids are drawn at the 50% probability level, except for the hydrogen atoms represented by spheres. The intermolecular hydrogen bonds are shown with dashed lines.

The comparison of the dimensions of **1** with the bond lengths and angles of similar structures accounted in the CSD [29] was performed by program Mogul 1.6 [30]. The *z*-score, which is the absolute difference between observed and mean values of a geometric parameter divided by the standard deviation of the Mogul distribution, to highlight unusual geometric features, is used in the program. A high value (e.g. >2.0) may indicate the specific structural feature. Only one unusual bond length d(O1–C15) = 1.494(3)

Table 1
Crystal data and structure refinement parameters.

Formula moiety	$C_{14}H_{22}N_2O_3S$
Molecular weight (g/mol)	298.39
Temperature (K)	296
Space group, *Z*	$P2_12_12_1$, 4
a (Å)	9.7454(4)
b (Å)	11.2225(4)
c (Å)	13.9171(5)
V (Å^3)	1522.1(1)
ρ_{calc} (g/cm^3)	1.302
μ (mm^{-1})	0.222
Reflections measured	18798
Reflections independent	4473
Reflections with $F > 4\sigma(F)$	3918
$2\theta_{max}$ (°)	60.168
h, *k*, *l* – limits	$-13 \le h \le 11$; $-15 \le k \le 15$; $-19 \le l \le 18$
R_{int}	0.0480
Refinement results	
The weighed refinement of F^2	$w = 1/[\sigma^2(F_o^2) + (0.0444P)^2 + 0.4465P]$ where $P = \max(F_o^2 + 2F_c^2)/3$
Number of refinement parameters	190
*R*1 [$F_o > 4\sigma(F_o)$]	0.0417
*wR*2	0.0950
Goof	1.034
$\Delta\rho_{max}$ (e/Å^3)	0.585
$\Delta\rho_{min}$ (e/Å^3)	−0.269
$(\Delta/\sigma)_{max}$	0.001

Table 2
Measured bond lengths and the values calculated by DFT for **1** [Å].

	Measured	Calculated
S–C2	1.672 (2)	1.683
O1–C4	1.340 (3)	1.342
O1–C15	1.494 (3)	1.477
O2–C6	1.241 (3)	1.224
O3–C15	1.390 (3)	1.394
N1–C2	1.376 (3)	1.375
N1–C6	1.412 (3)	1.426
N1–C7	1.486 (3)	1.483
N3–C2	1.377 (3)	1.390
N3–C4	1.385 (3)	1.387
N3–C9	1.484 (3)	1.487
C4–C5	1.359 (3)	1.364
C5–C6	1.426 (3)	1.445
C5–C11	1.521 (3)	1.530
C7–C8	1.515 (3)	1.527
C9–C10	1.520 (3)	1.527
C11–C14	1.535 (3)	1.548
C14–C15	1.503 (3)	1.520

Å (z-score = 2.23) was found in **1**. However, this bond length is only slightly higher than the maximum value 1.489 Å for such bond lengths observed in 28 similar motifs, and the motif number is small to get good statistics (Fig. 2S). As far as the refinement of crystal structure **1** is good, we can conclude that the maximal value of this bond in related motifs can be enlarged.

The structural analysis revealed one intermolecular O–H···O hydrogen bond which forms an infinity chain along the c-axis (Fig. 2, Table 3). Also, there are seven intramolecular hydrogen bonds C–H···S and C–H···O in the structure (Fig. 1, Table 3). According to the conventional classification such hydrogen bonds can be identified as weak hydrogen bonds [31]. They form four 5-member cycles [structural motif S(5)] like in MDETBA (M = Li, Na, K, Ag) and $Pb(DETBA)_2$ [26–28], and three 6-member cycles [structural motif S(6)] (Fig. 1). The C_2H_5 and CH_3 groups in **1** can rotate easily around the single C–C bond, but such ion form is stabilized due to these intramolecular hydrogen bonds. The search of π–π interaction between the heterocyclic rings using program PLATON [32] was unsuccessful.

The ethyl groups in HDETBA compounds can be on one side of the heterocycle (*cis*-conformer) plane and on the opposite sides of the plane (*trans*-conformer) [26–28,33]. The reasons for this behavior are not clear. The calculations show that *cis*- and *trans*-conformers are very close in energy [33]. It is known that HDETBA [17,18] exists in the *cis*-configuration. There is no information about the *trans*-isomer of pure HDETBA. However, it was found that several metal complexes of MDETBA form the *trans*-isomer of $DETBA^-$. Also, it was shown that the increase of alkaline ion radii leads to the fact that $DETBA^-$ ions become closer packed and consequently become *trans*-isomers [26]. The present investigation presents the compound with *trans*-configuration of the $DETBA^-$ molecule part appeared without forming metal complexes, as was found in compounds with codes FOWNIP, DAVKUI, GUDWEH and MUBCES in CSD [34]. It seems that the *cis*-configuration of **1** can also be crystallized. Moreover, from the geometrical point of view, such molecule can be stabilized by an additional C–H···O intramolecular hydrogen bond between $C10H_3$ group and the O3 atom (Fig. 1), but, unexpectedly, the *trans*-isomer becomes more stable. The reason for forming this *trans*-isomer can also be due to a high degree of molecular packing like in metal complexes and should be investigated wider.

For comparison, the crystal structure **2** (code HATZAD in CSD) [34], which is close to structure **1** and contains the bicyclic ring system, is presented in Fig. 3. The heterocyclic bases in **1** and **2** consist of the same atoms which are connected in the same sequence. The pyrimidine cycle in **1** is based on HDETBA, but, in **2**, it is based on 2-thiobarbituric acid. In contrast to **2**, there are no double bonds in the second ring of compound **1**. There are ≡C–OH in this cycle instead of >C=O and there are two additional $-CH_3$ groups. Thus, compound **1** has a previously unknown structural type of the bicyclic ring system based on thiobarbituric acids; it contains hydrophilic and hydrophobic groups and may possess a specific biological activity.

3.3. IR absorption spectrum of **1** in KBr

The IR absorption spectrum of **1** in KBr is rather structureless at the large and medium wavenumbers. The following bands were found in the IR absorption spectrum of **1**, as shown in Fig. 3S (cm^{-1}): 3395 s., 2982 m., 2957 w., 2925 w., 2874 w., 2563 vw., 2392 vw., 1644 vs., 1601 vs., 1446–1420 vs., 1390–1380 s., 1327 w., 1291 m., 1268 s., 1231 s., 1174 s., 1151 s., 1107 s., 1056 s., 992 w., 965 w., 918 w., 884 s., 857 m., 829 m., 807 s., 778 m., 751 vw., 704 w., 660 m., 625 w., 590 w., 550 w., 508 w., 484 vw., 468 vw., 452 vw., 430 w., 407 w. (vs. – very strong, s. – strong, m. – medium, w. – weak, vw. – very weak).

The abundance of overlapping bands complicates their assignment. The strong band at 1644 cm^{-1} in the IR spectra of HDETBA (Fig. 3S) was assigned previously to oscillation ν(C=O) [17]. The position of this band in the IR spectrum of **1** is almost unchanged,

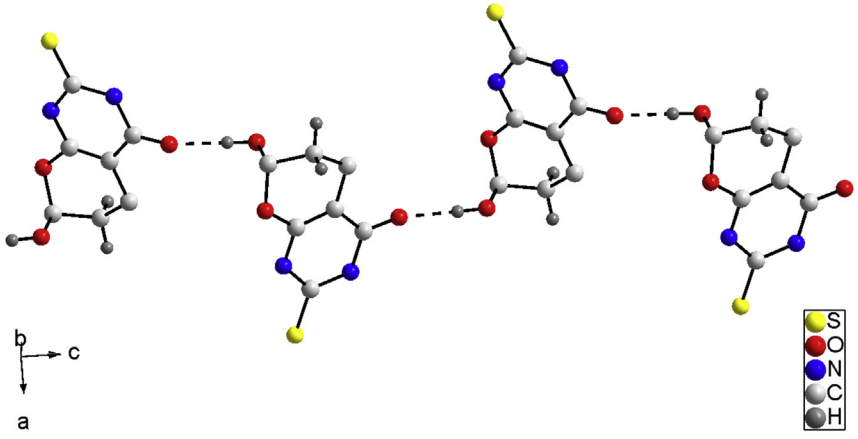

Fig. 2. The molecule chain along c-axis as formed by hydrogen bonds. The CH_3 and CH_2–CH_3 fragments are deleted for clarity.

Table 3
Hydrogen-bond geometry in the **1** (Å, 0).

D–H	d(D–H)	d(H···A)	∠ D–H···A	D···A	A	Transformation for A atom
O3–H3	0.92(4)	1.84(4)	173(3)	2.755(2)	O2	$3/2 - x, 1 - y, -1/2 + z$
C7–H7A	0.97	2.61	105	3.002(2)	S	x, y, z
C7–H7B	0.97	2.33	98	2.657(4)	O2	x, y, z
C9–H9A	0.97	2.57	106	2.983(2)	S	x, y, z
C9–H9B	0.97	2.24	102	2.613(3)	O1	x, y, z
C12–H12C	0.96	2.41	118	2.982(4)	O2	x, y, z
C13–H13A	0.96	2.58	120	3.166(3)	O2	x, y, z
C13–H13C	0.96	2.38	122	2.998(3)	O3	x, y, z

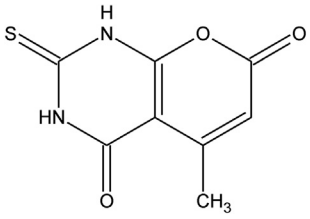

Fig. 3. Structure of 5-methyl-2-thioxo-1,2,3,4-tetrahydro-7*H*-pyrano[2,3-d]pyrimidine-4,7-dione methanole solvate $C_8H_6N_2O_3S \cdot CH_3OH$ (**2**).

but is accompanied by a strong band at 1601 cm^{-1}. These data are consistent with the presence of nonequivalent bonds C–O in the structure of **1**. The medium intensity band at 1151 cm^{-1} in the IR spectrum of **1**, which is specific for HDETBA and which was earlier attributed to ν(C=S) in 2-thiobarbituric acid [35,36] confirms the presence of thione group >C=S in **1**. The broad strong band at 3395 cm^{-1} is assigned to ν(O–H) vibrations. Thus, the results of IR spectroscopy are consistent with the structure of **1**, as obtained by X-ray diffraction.

3.4. The mass spectrometric analysis of *1*

The mass spectra of the acetone adducts of 1,3-diethyl-2-thiobarbituric acid MS *m/z* (%) 298 (M^+, 62), 283 (11), 241 (99), 240 (26), 215 (19), 207 (base peak, 100), 208 (16), 200 (46), 199 (18), 198 (21), 172 (30), 154 (47), 99 (28), 97 (17), 83 (26), 72 (33), 71 (25), 69 (31) showed first a molecular peak at $m/z = 298$, as evident in Fig. 4S. This peak may be assigned to compound **1** (Scheme 1). Several other strong peaks are attributed to different parts of this molecule (Fig. 4S) which may be considered as a further proof for the formation of the acetone adduct.

3.5. Theoretical studies

Initially, the structure optimization was carried out applying the B3LYP level of Density Functional Theory (DFT) [37] at the 6–311++G** basis set using program package Firefly v. 8.1.0. The calculated bond lengths are well related to those obtained from the results of the X-ray analysis, as shown in Table 2. The similar relation is also observed for the valence angles (Table 1S). The frontier orbitals (Highest Occupied Molecular Orbital (HOMO), Lowest Unoccupied Molecular Orbital (LUMO)) and transition energy levels calculated by DFT are shown in Fig. 4. The excitation energy value for the HOMO–LUMO transition was found as 4.8083 eV. The formation of π bonds by the interaction of p orbitals can be clearly seen in Fig. 4, in the HOMO view. It is difficult to interpret the IR-spectra of **1** empirically (Fig. 3S) because of a large number of overlapping bands. The quantum chemical calculations of IR spectra of the compound **1** monomer molecule and the estimation of the dimer formation energy via intermolecular hydrogen bond

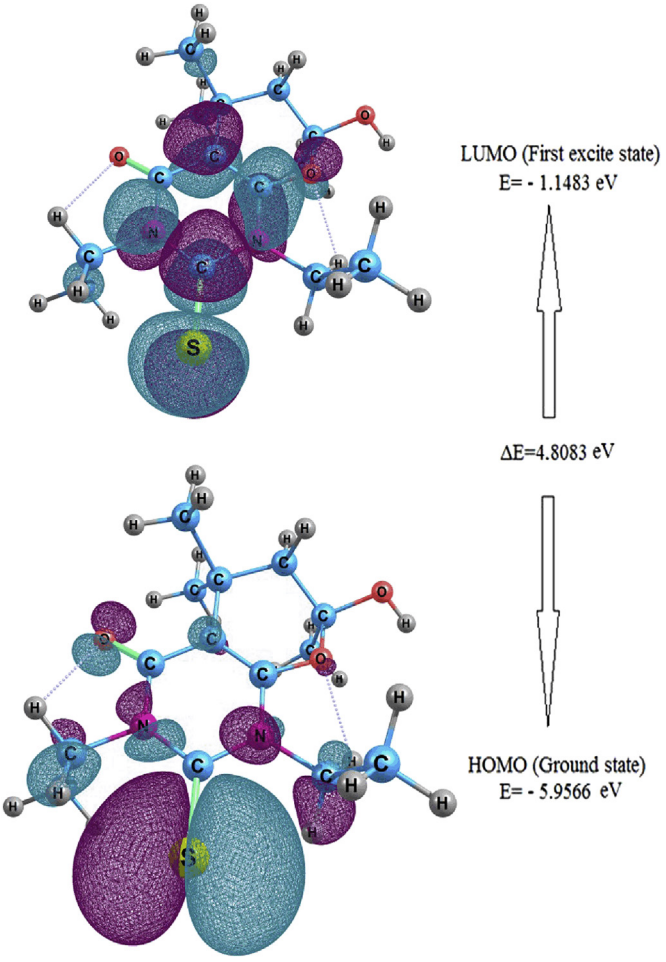

Fig. 4. View of the frontier orbitals (HOMO–LUMO) of the **1** and the energy levels.

O–H···O were implemented by the DFT (B3LYP/6–311 + G(d,p)) methods assisted with package GAUSSIAN-09 [38]. The experimental (in KBr and CCl_4) and theoretical wavenumbers of the IR spectrum of **1** are presented in Table 4. As it is evident from Table 4, the resulting assignment of the main bands in the IR spectrum is consistent with the results previously reported for HDETBA [17] and related 2-thiobarbituric acid [35,36].

The single monomer absorption band ν_{NH} at 3595 cm^{-1} is observed in the IR spectrum of compound **1** dilute solution in CCl_4 (Fig. 5). At the increase of concentration **1** in the solution, the intensity of the broad band centered at 3393 cm^{-1} increases and that is attributed to the self-association of molecules **1**. Comparatively, self-association band ν_{NH} at 3395 cm^{-1} is observed in the IR spectra of the crystallized compound **1** packed in KBr (Table 4). Spectral

Table 4
FTIR signals for **1** and comparison with the theoretical (B3LYP/6–311 + G**) in gas phase.

Experimental (cm^{-1})	Harmonic	Fundamental[a]	Assignment
3595 (CCl_4)	3805	3596	$\nu(OH)_{free}$
3395 (KBr)/3393 (CCl_4)			$\nu(OH)_{connected}$
2982 (KBr)	3155	2981	$\nu as(CH_2)$
2957 (KBr)	3142	2969	$\nu as(CH_3)$
2925 (KBr)	3114	2942	$\nu s(CH_2)$
2874 (KBr)	3029	2862	$\nu s(CH_2)$
1644 (KBr)	1711	1616	$\nu(C{=}O)$
1601 (KBr)	1644	1553	$\nu s(C{=}C)$
1446–1420 (KBr)	1521–1486	1423	$\delta as(CH_3)$
1390–1380 (KBr)	1482–1422	1378	$\delta as(CH_2)$
1291 (KBr)	1356	1282	$\delta s(CH_3)$
1268 (KBr)	1349	1271	$\delta s(CH_2)$
1231 (KBr)	1317	1244	$\nu as(C{-}O{-}C)$
1174 (KBr)	1257	1187	$\nu(C{-}N)$
1151 (KBr)	1212	1145	$\nu(C{=}S)$

[a] Obtained from the harmonic frequencies by multiplying by the scale factor of 0.945.

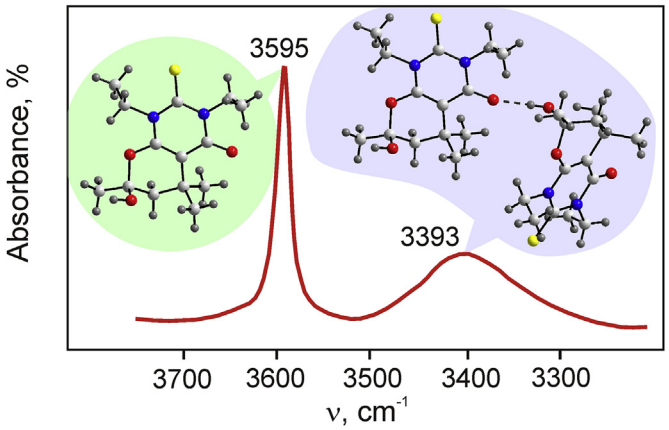

Fig. 5. IR spectra of solution **1** in CCl_4 in the region of stretching vibrations of OH groups.

shift $\Delta\nu = 200\ cm^{-1}$ indicates the formation of the solid crystal intermolecular hydrogen bonds. The dimer formation energy estimated by formula $E = 2E_{monomer} - E_{dimer}$ is equal to 7.5 kcal. The calculations showed that, in the gas phase, the dimer intermolecular hydrogen bond length is 1.848 Å, and the value practically coincides with that obtained from the X-ray diffraction analysis (1.841 Å). The strong band with the maximum at 268 nm is observed in the electronic absorption spectra (EAS) 2.2×10^{-5} M of the aqueous solution of **1**, as shown in Fig. 5S. For comparison, the EAS spectrum of **1** was calculated using TD-DFT. There are two characteristic peaks with the calculated wavenumber values of 281 and 268 nm, and these were attributed to the transitions in C=S groups in the thiobarbituric acid rings. The first peak at 281 nm is attributed to the $n \rightarrow \pi^*$ transition which is not observed in the experimental EAS spectrum, supposedly, due to low peak intensity. The second peak at 268 nm can be assigned to the $\pi \rightarrow \pi^*$ transition and it practically coincides with the experimental value (Fig. 5S). The dipole moment of the molecule is equal to 5.0451 D and the direction of the dipole moment is shown in Fig. 6S.

3.6. PASS results

The biological activity spectra of this compound and HDETBA were theoretically obtained by the PASS Online Program (http://www.way2drug.com/PASSOnline/). This software estimates the predicted activity spectrum of a compound as probable activity (Pa) and probable inactivity (Pi) [39]. The first 15 biological activity spectrum of 1 and HDETBA are represented in Table 2S. In Ref. [40], it was supposed that level Pa > 0.7 indicates that the corresponding compound is very likely to reveal activity in the experiments; 0.5 < Pa < 0.7 suggests that the compound is likely to reveal the activity in the experiments, while Pa < 0.5 implies that the compound is unlikely to reveal the activity in the experiments. Value Pa = 0.706 (Table 2S) indicates that compound **1** is very likely the Proteasome ATPase inhibitor and the same inhibitory effect for HDETBA is even more probable (Pa = 0.897). The pharmacological activity spectrum of **1** is about seven times narrower than that of HDETBA. Contrary to HDETBA, compound **1** exhibits specific activity to the CYP2H substrate (Pa = 0.693), antieczematic (Pa = 0.577), phosphatase inhibitor (Pa = 0.566), transcription factor NF kappa B stimulant (Pa = 0.508) and the transcription factor stimulant (Pa = 0.508) which deserves further consideration (Table 2S).

4. Conclusions

The novel 2-thiobarbituric acid derivative **1** containing a new bicyclic ring system was synthesized and characterized in the present study. Using the PASS software, the specific pharmacological activity of **1**, in comparison with HDETBA, was supposed. On the example of acetone, the method for synthesizing a new class of bicyclic compounds was proposed, which can be extended to other barbituric acids. It may also be applicable to the preparation of the compounds from barbiturates with other ketones and aldehydes. Moreover, the second cycle can be formed using C5 and O1 atoms of barbituric acid with two molecules of one type of ketone or aldehyde, as well as with two different types. Furthermore, such bicyclic structure may be formed by joining one molecule of ketone and aldehyde. One of the molecules of these carbonyl compounds with various substituents may be attached to HDETBA, in accordance with the condensation reaction of Knoevenagel which is usual for these compounds. Other molecule may be joined through the active α-carbon atom (with respect to the carbonyl group of the atom) to the residue of ketone or aldehyde associated with HDETBA. Formaldehyde does not contain an active α-carbon atom and, probably, its behavior is specific. Then, the nucleophilic attack of O1 atom of HDETBA on the carbon atom of the carbonyl group, which is not directly connected to a molecule of ketone or aldehyde, may close the additional 6-membered cycle with forming a bicyclic structure.

To establish the reaction mechanism, further research is needed. The scheme of the synthesis of **1** was suggested. It involves the formation of an intermediate product 5-(isopropylidene)-1,3-diethyl-2-thiobarbituric acid and its interaction with acetone, which is enolizated in the acidic solution (Scheme 1). Subsequently, **1** can participate in the condensation reaction with HDETBA and/or acetone and be a precursor of new substances with interesting and useful properties. In the present study, the *trans*-configuration of $DETBA^-$ part of molecule was obtained. Further investigation of the reaction and reaction products can be useful to understand why pure HDETBA exists only in the *cis*-configuration, or may be helpful to find the *trans*-configuration of HDETBA. It is supposed that the *cis*–isomer of compound **1** can be stabilized by the additional C–H···O intramolecular hydrogen bond between the $C10H_3$ group and O3, and also can be crystallized. The surprising stability of *trans*-isomer can be due to a high degree of molecular packing like in metal complexes and it should be investigated wider.

Acknowledgments

The work was carried out within the public task of the Ministry of Education and Science of the Russian Federation for research engineering of the Siberian Federal University in 2015 (Contract 3049). V.V.A. is grateful to the Ministry of Education and Science of the Russian Federation for the financial support of the investigation (Contract 14.607.21.0106). The authors also thank SFU CEJU for the technical support.

Appendix A. Supplementary data

Supplementary data related to this article can be found at http://dx.doi.org/10.1016/j.molstruc.2015.08.046.

References

[1] S. Bondock, T.A. El-Gaber, A.A. Fadda, Phosphorus Sulfur Silicon Relat. Elem. 182 (2007) 1915–1936.
[2] R. Ya Levina, F.K. Velichko, Russ. Chem. Rev. Engl. Transl. 29 (1960) 437.
[3] V.K. Ahluwalia, R. Aggarwal, Proc. Indian Nat. Sci. Acad. 5 (5) (1996) 369–413.
[4] J.H. Lee, S. Lee, M.Y. Park, H.J. Myung, Virol. J. 8 (2011) 18.
[5] V.I. Balas, I.I. Verginadis, G.D. Geromichalos, N. Kourkoumelis, L. Male, M.B. Hursthouse, K.H. Repana, E. Yiannaki, K. Charalabopoulos, T. Bakas, S.K. Hadjikakou, Eur. J. Med. Chem. 46 (7) (2011) 2835–2844.
[6] S. Vijaya Laxmi, Y. Thirupathi Reddy, B. Suresh Kuarm, P. Narsimha Reddy, P.A. Crooks, B. Rajitha, Bioorg. Med. Chem. Lett. 21 (2011) 4329–4331.
[7] N.R. Penthala, P.R. Ponugoti, V. Kasam, P.A. Crooks, Bioorg. Med. Chem. Lett. 23 (5) (2013) 1442–1446.
[8] K.M. Khan, F. Rahim, A. Khan, M. Shabeer, S. Hussain, W. Rehman, M. Taha, M. Khan, S. Perveen, M.I. Choudhary, Bioorg. Med. Chem. 22 (2014) 4119–4123.
[9] W.F. Smyth, G. Svehla, P. Zuman, Anal. Chim. Acta. 51 (3) (1970) 489–495.
[10] W.F. Smyth, G. Svehla, P. Zuman, Anal. Chim. Acta. 52 (1) (1970) 129–138.
[11] B.A. Ivin, V.I. Slesarev, N.A. Smorygo, Russ. J. Org. Chem. 10 (1974) 1968–1973.
[12] A.N. Razvi, A.H. Bakrya, S.M. Afzald, S.A. Khanb, A.M. Asiri, Mater. Lett. 144 (2015) 131–134.
[13] B.W. Domagalska, K.A. Wilk, H. Szymusiak, R. Zielin'ski, Comput. Chem. 24 (2000) 359–367.
[14] K. Rustemeier, D. Demetriou, G. Schepers, P. Voncken, J. Chromatogr. 613 (1993) 95–103.
[15] E.A. Munchow, L.L. Valente, S.L. Peralta, M.R. Fernandez, G.S. Lima, C.L. Petzhold, E. Piva, F.A. Ogliari, J. Biomed. Mater. Res. B Appl. Biomater. 101 (7) (2013) 1217–1221.
[16] O.A. Reutov, A.L. Kurtz, K.P. Butin, Organic Chemistry, Part 3, Binom, Moscow, 2004. ISBN 5-94774-110-5.
[17] J.P. Bideau, P.V. Huong, S. Toure, Acta Crystallogr. B32 (1976) 481–488.
[18] J.P. Bideau, P.V. Huong, S. Toure, Acta Crystallogr. B33 (1977) 3847–3849.
[19] M.S. Jovanovich, E.R. Biehl, J. Heterocycl. Chem. 24 (1987) 191–204.
[20] N.N. Golovnev, M.S. Molokeev, L.S. Tarasova, V.V. Atuchin, N.I. Vladimirova, J. Mol. Struct. 1068 (2014) 216–221.
[21] F. Oguz, I. Dogan, Spectrosc. Lett. 31 (2) (1998) 469–482.
[22] T.C. Lewis, D.A. Tocher, S.L. Price, Cryst. Growth Des. 4 (5) (2004) 979–987.
[23] G.M. Sheldrick, Acta Crystallogr. A64 (2008) 112–122.
[24] G.M. Sheldrick, SHELXL-97: A Program for Crystal Structure Refinement, University of Gottingen, Gottingen, Germany, 1997.
[25] A.A. Dvorkin, S.G. Soboleva, J.A. Simonov, S.A.C.A. Andronati, T.I. Malinovskii, Dokl. Akad. Nauk. SSSR Dan. SSSR 262 (1982) 99–103.
[26] N.N. Golovnev, M.S. Molokeev, S.N. Vereshchagin, I.V. Sterkhova, V.V. Atuchin, Polyhedron 85 (2015) 493–498.
[27] N.N. Golovnev, M.S. Molokeev, I.I. Golovneva, Russ. J. Coord. Chem. 41 (5) (2015) 300–304.
[28] N.N. Golovnev, M.S. Molokeev, M.A. Lutoshkin, Russ. J. Inorg. Chem. 60 (5) (2015) 572–576.
[29] F.H. Allen, Acta Crystallogr. B58 (2002) 380–388.
[30] Mogul 1.6, Cambridge Crystallographic Data Centre, 2003–2012.
[31] J.W. Steed, J.L. Atwood, Supramolecular Chemistry, first ed., CRC Press, Moscow, 2007, 2004, IKTs Akademkniga.
[32] PLATON – A Multipurpose Crystallographic Tool, Utrecht University, Utrecht, The Netherlands, 2008.
[33] R. Notario, M.V. Roux, F. Ros, V.N. Emel'yanenko, D.H. Zaitsau, S.P. Verevkin, J. Chem. Thermodyn. 77 (2014) 151–158.
[34] B. Viossat, N.-H. Dungt, A. Tomas, A. Esanu, A. Rolland, Acta Cryst. C50 (1994) 269–271.
[35] N.A. Smorygo, B.A. Ivin, Khim. Geterotsikl. Soedin. 10 (1975) 1402.
[36] E. Mendez, M.F. Cerda, J.S. Gancheff, J. Torres, C. Kremer, J. Castiglioni, M. Kieninger, O.N. Ventura, J. Phys. Chem. C 111 (2007) 3369–3383.
[37] P. Hohenberg, W. Kohn, Phys. Rev. 136 (1964) B864–B871.
[38] M.J. Frisch, G.W. Trucks, H.B. Schlegel, G.E. Scuseria, M.A. Robb, J.R. Cheeseman, G. Scalmani, V. Barone, B. Mennucci, G.A. Petersson, H. Nakatsuji, M. Caricato, X. Li, H.P. Hratchian, A.F. Izmaylov, J. Bloino, G. Zheng, J.L. Sonnenberg, M. Hada, M. Ehara, K. Toyota, R. Fukuda, J. Hasegawa, M. Ishida, T. Nakajima, Y. Honda, O. Kitao, H. Nakai, T. Vreven, J.A. Montgomery Jr., J.E. Peralta, F. Ogliaro, M. Bearpark, J.J. Heyd, E. Brothers, K.N. Kudin, V.N. Staroverov, R. Kobayashi, J. Normand, K. Raghavachari, A. Rendell, J.C. Burant, S.S. Iyengar, J. Tomasi, M. Cossi, N. Rega, J.M. Millam, M. Klene, J.E. Knox, J.B. Cross, V. Bakken, C. Adamo, J. Jaramillo, R. Gomperts, R.E. Stratmann, O. Yazyev, A.J. Austin, R. Cammi, C. Pomelli, J.W. Ochterski, R.L. Martin, K. Morokuma, V.G. Zakrzewski, G.A. Voth, P. Salvador, J.J. Dannenberg, S. Dapprich, A.D. Daniels, O. Farkas, J.B. Foresman, J.V. Ortiz, J. Cioslowski, D.J. Fox, Gaussian 09, Revision A.01, Gaussian, Inc., Wallingford CT, 2009.
[39] D.A. Filimonov, V.V. Poroikov, Probabilistic Approach in Activity Prediction, RSC Publishing, Cambridge, 2008, pp. 182–216.
[40] D.A. Filimonov, A.A. Lagunin, T.A. Gloriozova, A.V. Rudik, D.S. Druzhilovskii, P.V. Pogodin, V.V. Poroikov, Chem. Heterocycl. Compd. 50 (3) (2014) 444–457.